23rd ABCM International Congress of Mechanical Engineering
December 6-11, 2015, Rio de Janeiro, RJ, Brazil

MOTION CONTROL OF AN UNDERACTUATED WHEELED MOBILE ROBOT: A KINEMATIC INPUT-OUTPUT LINEARIZATION APPROACH

Werther Alexandre de Oliveira Serralheiro
Newton Maruyama
Eduardo Aoun Tannuri
Departamento de Engenharia Mecatrônica e de Sistemas Mecânicos
Escola Politécnica da Universidade de São Paulo
Av. Prof. Mello Moraes, 2231, São Paulo, Brasil
e-mails:{werther,maruyama,eduat}@usp.br

Abstract. *This work addresses a trajectory tracking controller for the kinematics of an underactuated wheeled mobile robot, in environments without obstacles, using input-output linearization and the Follow the Carrot algorithm. The use of input-output linearization allows the reduction of error dynamics into a linear order system. In this case, the controller is expressed as a* 2×2 *diagonal gain matrix. Different types of trajectories are devised in order to analyse the feasibility of the method. A specific trajectory consisting of a mix of smooth and sharp curvature sections is utilized in order to investigate the sensitivity of the control system in relation to gain variations. Some novelty is claimed by authors in relation to the use of kinematic input-output linearization combined to the Follow the Carrot algorithm.*

Keywords: *wheeled mobile robots, trajectory tracking, motion control, nonlinear control system, input-output linearization.*

1. Introduction

Over the last few decades the research on motion control of mobile robots has been rapidly increasing. Under motion control it is possible to identify three basic problems:

- Point stabilization: the vehicle is required to stabilize at a given pose (position and orientation);
- Path following: the vehicle is required to follow a given geometric path;
- Trajectory tracking: the vehicle is required to track a trajectory, i.e., a geometric path with temporal properties.

Since there is no temporal specification in the path following problem, the performance is expressed by the minimum distance d from the vehicle to the geometric path. In the trajectory tracking problem the control system performance is expressed by the distance e from the vehicle to a reference point as shown on Figure 1.

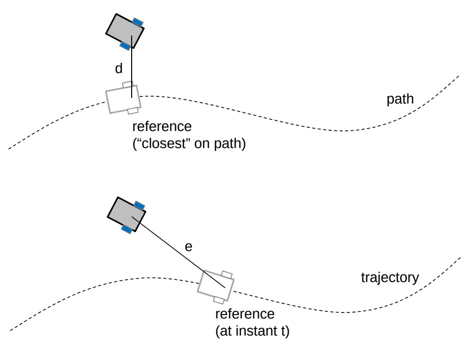

Figure 1. Path following versus Trajectory tracking.

Several path following and trajectory tracking control algorithms have been described in the mobile robotics literature (Svec *et al.*, 2014). Classical methods, such as the *Follow the Carrot* (Barton, 2001) and the *Pure Pursuit* (Coulter, 1992), use robot position information to compute steering commands in order to follow a predefined geometric path. Variations of these algorithms are also found in the literature, see for example, (Hogg *et al.*, 2002) and (Sujit *et al.*, 2013). These algorithms are known to have poor performance in corners since they do not take into account the actual curvature of the path.

More complex algorithms have been developed recently. The *Follow the Past* (Hellstrom and Ringdahl, 2006) uses recorded steering commands information to overcome the problem with sharp trajectory tracking found in the classical methods; the *Vector Pursuit* (Wit *et al.*, 2004; Yeu *et al.*, 2006) is a geometric path following method based on the screw theory; the *Valued-based controller* (Bohren *et al.*, 2008) integrates the dynamics of the vehicle model in order to predict optimal steering commands; a robust *Model Reference Adaptive Controller* has also been studied for mobile robots with uncertainties in the dynamical model (Aneesh, 2012).

Encarnação and Pascoal (2002) has introduced a combined trajectory tracking and path following control approach for wheeled robots. Other examples are (Aguiar and Hespanha, 2007; Xiang *et al.*, 2011; Alessandretti *et al.*, 2013).

This work addresses a trajectory tracking controller for the kinematics of an underactuated wheeled mobile robot, using feedback linearization and a typical motion control scheme: the *Follow the Carrot* algorithm. Although feedback linearization has been proposed in motion control of WMR (Kim and Oh, 1999; Oriolo *et al.*, 2002; Chwa, 2010; Akbati and Cansever, 2013), this paper claims novelty while combining kinematics feedback linearization and the Follow the Carrot algorithm.

The paper is organized as follows. In Section 2, a kinematic model formulation of a WMR is introduced. A control system scheme using feedback linearization and the Follow the Carrot approach is presented in Section 3. In Section 4, some simulation results are presented and discussed. Finally in Section 5 some conclusions about the feasibility of the proposed method are drawn.

2. The kinematic model

A differential wheeled mobile robot (WMR) is made up of a rigid frame and equipped with nondeformable driven wheels, as illustrated by the schematic diagram on Figure 2, where b is the vehicle width, l is the vehicle length and r the vehicle wheels radii.

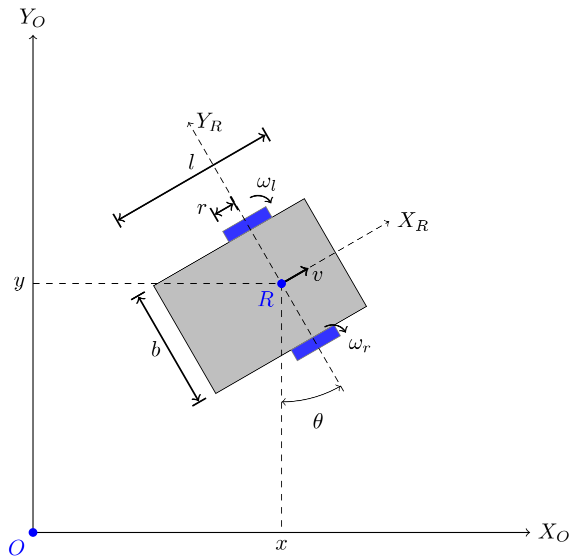

Figure 2. The differential WMR and the coordinate frames.

It is assumed that the robot is moving on a horizontal plane and an arbitrary inertial frame $\{O\} = \{X_O, Y_O\}$ is fixed in the motion plane. The robot coordinate frame $\{X_R, Y_R\}$ is attached to the robot chassis on the reference point given by R, which is positioned in the middle of the shaft. The position coordinates of R in relation to the inertial frame is given by x and y, and the rotation angle between both coordinates frames is given by θ. The WMR pose is then completely defined by the following vector:

$$\boldsymbol{\xi_O}(t) = [x(t)\; y(t)\; \theta(t)]^T. \tag{1}$$

As both wheels are individually controlled it results that the angular wheel velocities $\omega_r(t)$ e $\omega_l(t)$ are independent. Their relationship with the robot translation velocity $v(t)$ and with the angular velocity $\dot{\theta} = \omega(t)$ can be written by the following equations (Nørgaard *et al.*, 2000):

$$
\begin{aligned}
v(t) =& \frac{r(\omega_r(t) + \omega_l(t))}{2} \\
\omega(t) =& \frac{r(\omega_r(t) - \omega_l(t))}{b}
\end{aligned}
\tag{2}
$$

The velocities of R in the inertial coordinate frame $\{O\}$ are given by $\dot{x}(t) = v(t)cos\theta(t)$ and $\dot{y}(t) = v(t)sen\theta(t)$. Then, the pose time derivative (kinematic model) can be written to yield:

$$
\dot{\boldsymbol{\xi}}_{\boldsymbol{O}} = \begin{bmatrix} \dot{x}(t) \\ \dot{y}(t) \\ \dot{\theta}(t) \end{bmatrix} = \begin{bmatrix} rcos\theta(t)/2 & rcos\theta(t)/2 \\ rsin\theta(t)/2 & rsin\theta(t)/2 \\ r/b & -r/b \end{bmatrix} \begin{bmatrix} \omega_r(t) \\ \omega_l(t) \end{bmatrix}
\tag{3}
$$

Note that the unicycle is underactuated, since $\dot{\boldsymbol{\xi}}_{\boldsymbol{O}} \in \mathbb{R}^3$ and the control signal $\boldsymbol{u} = [\omega_r(t)\ \omega_l(t)]^T \in \mathbb{R}^2$.

3. The control system

3.1 Feedback Linearization

The feedback linearization approach (Slotine and Li, 1991) is based on the cancelling of system nonlinearities while imposing desired linear dynamics. The central idea is to algebraically transform nonlinear system dynamics into fully or partly linear ones, so that linear control techniques might be applied.

Let a system described by the *companion form* as $\dot{\boldsymbol{x}} = f_1(\boldsymbol{x}) + f_2(\boldsymbol{x})\boldsymbol{u}$, where $\boldsymbol{u} \in \mathbb{R}^p$ is the control input, $\boldsymbol{x} \in \mathbb{R}^n$ is the state vector and $f_1(\boldsymbol{x})$ and $f_2(\boldsymbol{x})$ are nonlinear function of states. Using the control input given by:

$$
\boldsymbol{u} = (f_2)^{-1} \left[\boldsymbol{v} - f_1\right],
\tag{4}
$$

and if f_2 is not singular the nonlinearities can be cancelled and an input-output relation $\dot{\boldsymbol{x}} = \boldsymbol{v}$ is obtained. The control law $\boldsymbol{v}$ must be chosen such that the internal dynamics becomes stable. This linearization approach has been efficiently applied for WMR motion control, see for example (D'Andrea-Novel *et al.*, 1992; Kim and Oh, 1999; Oriolo *et al.*, 2002; Chwa, 2010).

3.2 The Follow the Carrot scheme

The WMR trajectory tracking consists in calculating the robot velocity and heading in order to force the robot to follow a predefined pose set. The *Follow the Carrot* (Barton, 2001; Sujit *et al.*, 2013) trajectory tracking approach originates from the idea of holding a carrot in front of a horse to force the animal to move in desired direction.

$C_p = (x_{ref}, y_{ref}) \in \{O\}$ is the coordinates of the Carrot Point moving in a predefined time parametrized and obstacle free geometric path[1]. The vector v_{cp} represents the Carrot Point velocity in the plane. A virtual segment line is drawn from the center $R = (x, y) \in \{O\}$ of the WMR to the Carrot Point C_p. Also a distance gap ρ within the same virtual segment line is considered to avoid singularity problems.

Based on these considerations, two errors are here defined the linear error e_l from the WMR to the distance gap ρ; and the heading error (e_θ) between the WMR direction and the Carrot Point C_p, as illustrated by Figure 3.

The components of the linear error in the X_O and the Y_O directions are respectively given by $e_x = (x_{ref} - x)$ and $e_y = (y_{ref} - y)$. Then, the errors e_l and e_θ can be written as:

$$
\begin{aligned}
e_l =& \sqrt{e_x^2 + e_y^2} - \rho, \\
e_\theta =& tan^{-1}\left(\frac{e_y}{e_x}\right) - \theta.
\end{aligned}
\tag{5}
$$

And the error derivatives become:

$$
\begin{aligned}
\dot{e}_l =& \frac{e_x(\dot{x}_{ref} - \dot{x}) + e_y(\dot{y}_{ref} - \dot{y})}{e_l}, \\
\dot{e}_\theta =& \frac{e_x(\dot{y}_{ref} - \dot{y}) - e_y(\dot{x}_{ref} - \dot{x})}{e_l^2} - \dot{\theta}.
\end{aligned}
\tag{6}
$$

[1] the explicit functional dependency on time t is neglected here in order to simplify the equations.

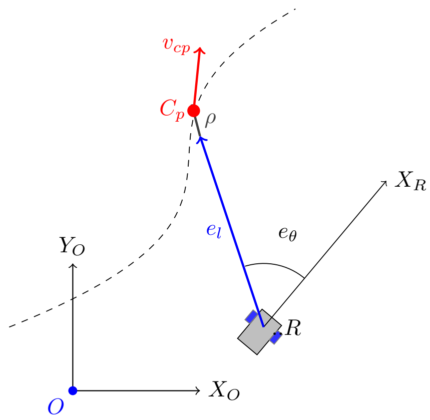

Figure 3. The Follow the Carrot scheme.

Substituting the kinematic unicycle model given by the Equation 3 into the Equation 6 and after some algebraic manipulations yields:

$$\left[\begin{array}{c}\dot{e}_l\\ \dot{e}_\theta\end{array}\right] = f_{1R}\left[\begin{array}{c}\dot{x}_{ref}\\ \dot{y}_{ref}\end{array}\right] + f_2\left[\begin{array}{c}\omega_r\\ \omega_l\end{array}\right], \tag{7}$$

where the nonlinear functions are given by:

$$\begin{aligned} f_{1R} &= \begin{bmatrix} +\left(\frac{e_x}{e_l}\right) & +\left(\frac{e_y}{e_l}\right) \\ -\left(\frac{e_y}{e_l^2}\right) & +\left(\frac{e_x}{e_l^2}\right) \end{bmatrix}, \\ f_2 &= \begin{bmatrix} -\mathfrak{A} & -\mathfrak{A} \\ -\mathfrak{B} - \frac{r}{b} & -\mathfrak{B} + \frac{r}{b} \end{bmatrix}. \end{aligned} \tag{8}$$

With the terms inside the f_2 matrix given by:

$$\begin{aligned} \mathfrak{A} &= \left[\frac{r}{2e_l}\left(e_x cos\theta + e_y sin\theta\right)\right], \\ \mathfrak{B} &= \left[\frac{r}{2e_l^2}\left(e_x sin\theta - e_y cos\theta\right)\right]. \end{aligned} \tag{9}$$

The control output becomes:

$$\left[\begin{array}{c}\omega_r\\ \omega_l\end{array}\right] = f_2^{-1}\cdot\left(K\left[\begin{array}{c}e_l\\ e_\theta\end{array}\right] - f_{1R}\left[\begin{array}{c}\dot{x}_{ref}\\ \dot{y}_{ref}\end{array}\right]\right), \tag{10}$$

where $K = \left(\begin{smallmatrix} K_l & 0 \\ 0 & K_\theta \end{smallmatrix}\right)$ is a diagonal matrix of gains. The dynamics of errors become:

$$\left[\begin{array}{c}\dot{e}_l\\ \dot{e}_\theta\end{array}\right] = K\left[\begin{array}{c}e_l\\ e_\theta\end{array}\right] \tag{11}$$

The errors e_l and e_θ converge to zero if and only if the eigenvalues of K are negative.

3.3 Computational implementation

The kinematic model Equation 3 is implemented as an open loop system, with the geometric parameters vehicle chosen as width $b = 0.3m$ and wheel radius $r = 0.1m$. A predefined time parametrized trajectory defines $[x_{ref}(t)\ y_{ref}(t)]^T$, with a time discretization of $\delta t = 0.05s$.

Each one the errors e_x, e_y, e_l and e_θ are calculated, as well as the time derivatives of the reference trajectory $[\dot{x}_{ref}(t)\ \dot{y}_{ref}(t)]^T$. A distance gap $\rho = 0.05m$ is chosen. Then, the closed loop system is calculated utilizing the Equation 10.

The complete closed loop control system is illustrated as a block diagram in Figure 4.

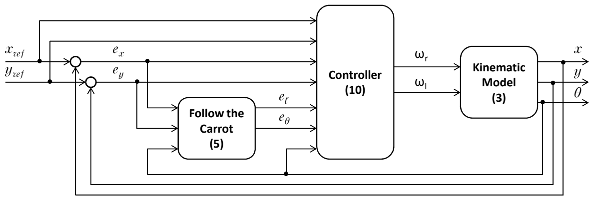

Figure 4. Closed loop system block diagram. The numbers inside the blocks refer to the reference numbers of equations.

4. Experimental results

This section illustrates some experimental results. Initially, with the gain matrix tuned as $K = \begin{pmatrix} -0.1 & 0 \\ 0 & -2.0 \end{pmatrix}$, some trajectories are tested as illustrated in Figure 5: a straight line and a circular pattern, both with constant velocity; a sinusoidal pattern with velocity component in the y direction constant and a spiral trajectory with exponential velocity.

In all performed simulations, the WMR motion reaches predefined geometrical paths and tracks the reference which is defined by the movement of the Carrot Point C_P. Furthermore, a specific trajectory, with a mix of smooth and sharp curvature sections, is chosen in order to foster discussions about the effectiveness of this approach. The trajectory tracking simulation results are illustrated in Figure 6. It is possible to note that after some transient period the geometric path is tracked satisfactorily.

In order to analyse the sensitivity of the control system to the variations of the gain matrix K two sets of simulations are conducted. In the first set of simulations the linear error gain is set to $K_l = -0.1$ while the heading angle error gain

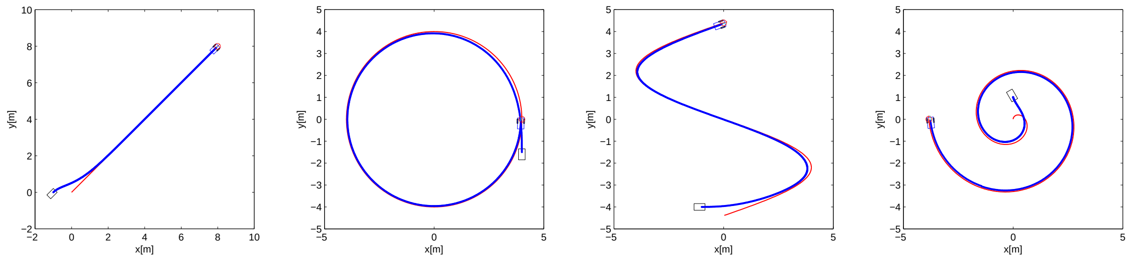

Figure 5. Tested trajectories. The red line represents the desired geometric path and the blue line represents the WMR motion behavior.

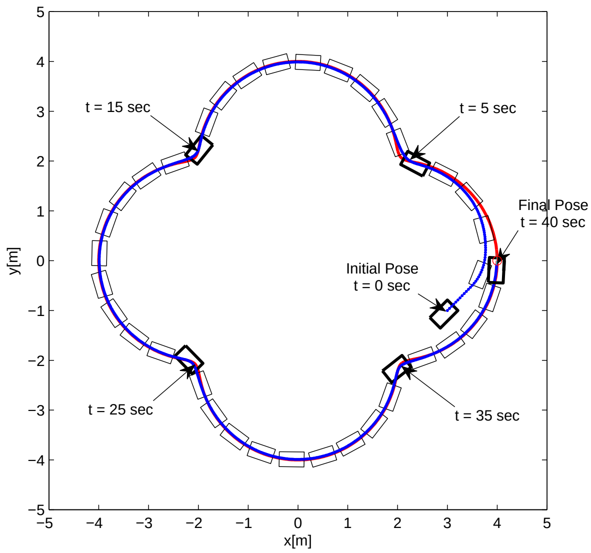

Figure 6. A specific trajectory with smooth and sharp curvature sections. Selected gains are $K_l = -0.1$ and $K_\theta = -10.0$.

K_θ is varied within the set $[-1.0, -5.0, -10.0, -35.0]$. The experimental results are illustrated in Figure 7.

In the upper part of Figure 7 the plot (a) shows the linear error e_l. All four curves for the linear error e_l are very close which indicates that for the chosen gain $K_l = -0.1$ the linear error dynamics is decoupled from the dynamics of the heading angle error e_θ. One must note that sharp curvature sections arise on time instants $t = 5sec$, $t = 15sec$, $t = 25sec$ and $t = 35sec$.

In the bottom part of Figure 7 the plot (b) illustrates the heading angle error e_θ. Overall, the heading angle error e_θ remains relatively small ($< 0.5rad$) but increases with the increase of time and oscillates in the sharp curvature sections. While increasing the module of the heading angle gain K_θ, the error decreases. However, for $K_\theta = -35$ bounded high frequency chattering signals are observed.

In the second set of simulations the linear error gain is varied within the set $K_l = [-0.1, -0.2, -0.5, -1.0]$ while the heading angle error gain is set to $K_\theta = -10.0$. The experimental results are illustrated in Figure 8.

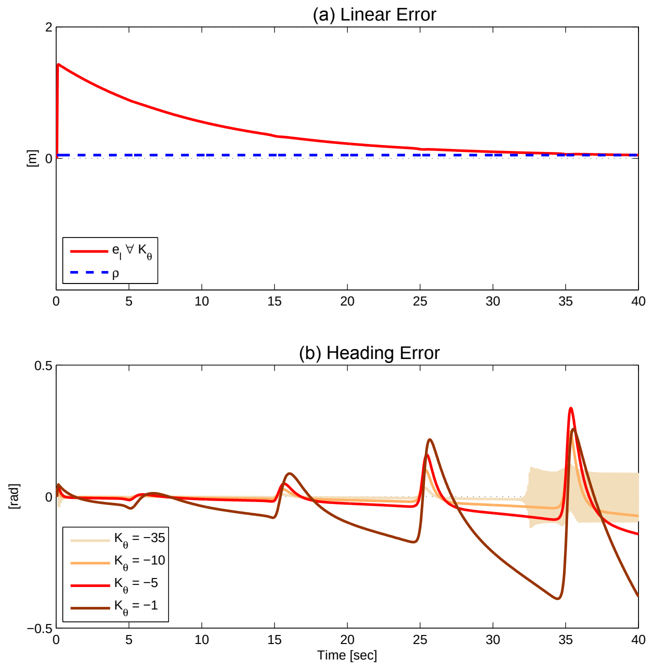

Figure 7. The (a) Linear error e_l and (b) the heading angle error e_θ for $K_l = -0.1$ and $K_\theta = [-1.0, -5.0, -10.0, -35.0]$.

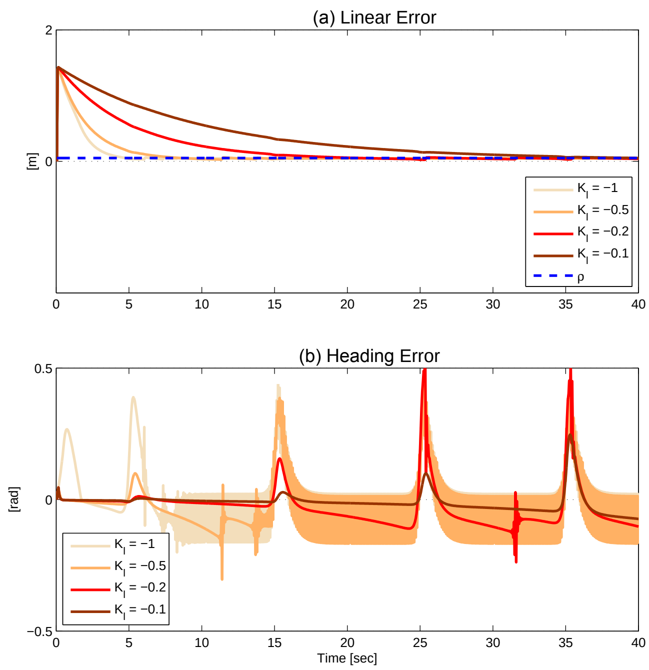

Figure 8. The (a) Linear error e_l and (b) the heading angle error e_θ for $K_l = [-0.1, -0.2, -0.5, -1.0]$ and $K_\theta = -10.0$.

In the upper part of Figure 8 the plot (a) shows the linear error e_l. It is possible to note that as the linear error gain K_l increases the transient response becomes faster with asymptotic behaviour. In the bottom part of Figure 8 the plot (b) shows the heading angle error e_θ. On the contrary, as the linear error gain K_l increases the heading angle error e_θ increases and becomes oscilattory and even with bounded high frequency chattering signals, specially for $K_l = -0.5$ and -1.0.

5. Conclusions and future work

In this work, a trajectory tracking control system for the kinematics of an underactuated wheeled mobile robot has been proposed. The main rationale is related to the use of feedback linearization and the *Follow the Carrot* algorithm.

The Follow the Carrot algorithm is based on forcing the WMR to track the trajectory defined by the movement of a Carrot point C_p. The control system performance is defined by a 2-dimensional error vector, whose components are the linear error e_l and the heading error e_θ.

The use of feedback linearization allows the dynamics of the error vector to become linear. The controller is expressed as a 2×2 diagonal matrix whose elements in the main diagonal are the gains K_l for the linear error e_l and K_θ for the heading angle error e_θ. The control system design is then reduced on the choice of K_l and K_θ.

Some experimental results have been obtained via computing simulations using the Simulink/Matlab environment. Some examples of trajectories have been defined for the experiments: a straight line and a circular pattern, both with constant velocity; a sinusoidal pattern with velocity component in the y direction constant and a spiral trajectory with exponential velocity. It has been shown that with chosen gains $K_l = -0.1$ and $K_\theta = -2.0$ the trajectories are tracked very satisfactorily.

In order to investigate the sensitivity of the control system to variations of gains K_l and K_θ a more challenging trajectory is proposed with a mix of smooth and sharp curvature sections. Two set of simulations are devised. In the first set of simulations K_l remains constant while K_θ varies. It is observed that the performance of the linear error e_l is robust against variations of K_θ but the performance of the heading angle error e_θ decreases with the increase of the module of K_θ

In the second set of simulations K_θ remains constant while K_l varies. It is possible to note that as the linear error gain K_l increases the transient response becomes faster with asymptotic behaviour. The performance of the heading angle error e_θ decreases with the increase of the linear error gain K_l.

In principle it seems that the linear error e_l is decoupled from the heading error e_θ but the opposite is not true. A more detailed analysis is required. Therefore, future work must comprise a more detailed analytical investigation about system instability. And also the dynamic part of the WMR model must be incorporated for a more realistic analysis of the control system performance.

6. ACKNOWLEDGEMENTS

This research is being developed under the Inter institutional Doctoral Research Program, between the IFSC (Instituto Federal de Santa Catarina) and the EPUSP (Escola Politécnica da Universidade de São Paulo), sponsored by the Coordenação de Aperfeiçoamento de Pessoal de Nível Superior (CAPES). Authors would like to acknowledge the support of the IFSC, the EPUSP and the CAPES.

7. REFERENCES

Aguiar, A. and Hespanha, J., 2007. “Trajectory-tracking and path-following of underactuated autonomous vehicles with parametric modeling uncertainty”. Vol. 52, No. 8, pp. 1362–1379.

Akbati, O. and Cansever, G., 2013. “Control of pattern tracking nonholonomic mobile robot with feedback linearization”. *IEEE International Conference on Electrical and Electronics Engineering*, , No. 2, pp. 512–515.

Alessandretti, A., Aguiar, A. and Jones, C.N., 2013. “Trajectory-tracking and path-following controllers for constrained underactuated vehicles using Model Predictive Control”. In *European Control Conference*. pp. 1371–1376.

Aneesh, D., 2012. “Tracking Controller of mobile robot”. In *International Conference on Computing, Electronics and Electrical Technologies*. 4.

Barton, M., 2001. *Controller development and implementation for path planning and following in an autonomous urban vehicle*. Thesis, University of Sydney.

Bohren, J., Foote, T. and Keller, J., 2008. “Little Ben: The Ben Franklin racing team’s entry in the 2007 Darpa urban challenge”. *Journal of Field Robotics*, Vol. 25, No. 9, pp. 598–614.

Chwa, D., 2010. “Tracking Control of Differential-Drive Wheeled Mobile Robots Using a Backstepping-Like Feedback Linearization”. *IEEE Transactions on Systems, Man, and Cybernetics - Part A: Systems and Humans*, Vol. 40, No. 6, pp. 1285–1295.

Coulter, R.C., 1992. “Implementation of the pure pursuit path tracking algorithm”. Technical Report CMU-RI-TR-92-01, Robotics Institute, Pittsburgh, PA.

D'Andrea-Novel, B., Bastin, G. and Campion, G., 1992. "Dynamic feedback linearization of nonholonomic wheeled mobile robots". In *IEEE International Conference on Robotics and Automation*. pp. 2527–2532.

Encarnação, P. and Pascoal, A., 2002. "Combined trajectory tracking and path following control for dynamic wheeled mobile robots". In *IFAC World Congress*.

Hellstrom, T. and Ringdahl, O., 2006. "Follow the Past: a path-tracking algorithm for autonomous vehicles". *International Journal of Vehicle Autonomous Systems*, Vol. 4, No. 2-4, pp. 216–224.

Hogg, R., Rankin, A., Roumeliotis, S., McHenry, M., Helmick, D., Bergh, C. and Matthies, L., 2002. "Algorithms and sensors for small robot path following". In *IEEE International Conference on Robotics and Automation*. Ieee, Vol. 4, pp. 3850–3857.

Kim, D.H. and Oh, J.H., 1999. "Tracking control of a two-wheeled mobile robot using input–output linearization". *Control Engineering Practice*, Vol. 7, No. 3, pp. 369–373.

Nørgaard, M., Poulsen, N. and Ravn, O., 2000. "Models for Iau's Autonomous Guided Vehicle". Technical report, Dept. of Mathematical Modelling - Technical University of Denmark, Lyngby.

Oriolo, G., De Luca, a. and Vendittelli, M., 2002. "WMR control via dynamic feedback linearization: design, implementation, and experimental validation". *IEEE Transactions on Control Systems Technology*, Vol. 10, No. 6, pp. 835–852.

Slotine, J. and Li, W., 1991. *Applied nonlinear control*. Prentice-Hall, Englewood Cliffs.

Sujit, P., Saripalli, S. and Sousa, J., 2013. "An evaluation of UAV path following algorithms". *European Control Conference*, , No. 1, pp. 3332–3337.

Svec, P., Thakur, A., Raboin, E., Shah, B.C. and Gupta, S.K., 2014. "Target following with motion prediction for unmanned surface vehicle operating in cluttered environments". *Autonomous Robots*, Vol. 36, No. 4, pp. 383–405.

Wit, J., Crane, C.D. and Armstrong, D., 2004. "Autonomous ground vehicle path tracking". *Journal of Robotic Systems*, Vol. 21, No. 8, pp. 439–449.

Xiang, X., Lapierre, L., Liu, C. and Jouvencel, B., 2011. "Path tracking: Combined path following and trajectory tracking for autonomous underwater vehicles". In *IEEE/RSJ International Conference on Intelligent Robots and Systems*. Ieee, pp. 3558–3563.

Yeu, T., Park, S. and Hong, S., 2006. "Path tracking using vector pursuit algorithm for tracked vehicles driving on the soft cohesive soil". In *SICE-ICASE*. pp. 2781–2786.

8. RESPONSIBILITY NOTICE

The authors are the only responsible for the printed material included in this paper.